JOURNAL OF MATERIALS SCIENCE 28 (1993) 669–676

Phase relationship between β′- and O′-sialon at 1623 K

H. WADA, M. J. WANG
Department of Materials Science and Engineering, University of Michigan, Ann Arbor, MI 48109, USA

β′-sialon whiskers and co-products of synthesis, such as β′-sialon powders and O′-sialon powders, were annealed at 1623 K for 8 h in a closed graphite reaction tube under 1 atm nitrogen. Phase stabilities, Si/Al ratios, and crystallographic features were investigated. The O′-sialon phase, which formed in the early stage of synthesis when oxygen partial pressure was relatively high, became less stable in the present annealing condition and decomposed. The majority of released aluminium and possibly oxygen from the decomposed O′-powder was incorporated into β′-sialon whiskers with little change in its lattice parameters, when the β′-sialon whiskers were included in annealing. The aluminium contents were always lower in the β′-whiskers than in the powders even after increasing its aluminium content during 8 h annealing. The lattice parameters of both β′-whiskers and powders increased with increasing aluminium content and became closer after annealing. The lattice parameters of β′-whiskers remained the same before and after annealing despite the increased aluminium content, while the lattice parameters of β′-powders decreased despite its aluminium content remaining unchanged. The lattice parameters of O′-sialon increased with increasing aluminium content, and the increase in the ***a*** direction is the largest when compared with other parameters.

1. Introduction

β′-sialon whiskers have been synthesized by a carbothermal reduction of silica at a relatively low temperature, 1623 K [1–4]. The whiskers were formed through a gas-phase reaction involving SiO(g), the generation of which was enhanced by the application of a low-viscosity molten bath containing either Na_3AlF_6 or NaF [1–4]. During the synthesis of β-silicon nitride, silicon oxynitride and α-silicon nitride were also formed in different areas of the reaction tube. Fig. 1 shows the cross-section of a graphite reaction tube which contains a powder bed of starting materials. Four sampling areas were assigned for the tube as Areas 1–4. Phases found in each area are shown in Fig. 1 for two different molten baths. When Na_3AlF_6 was used as the molten bath, α′-, β′- and O′-sialons were formed, while α-, β-Si_3N_4 and Si_2N_2O were formed when NaF was used.

Formation of Si_2N_2O or O′-sialon is limited in Area 4, and has been linked to the gas-phase composition particularly with a high p_{O_2} and a localized high $[p_{SiO}/p_{N_2}]$ ratio in Area 4 [3, 5]. The structure of Si_2N_2O is a three-dimensional network linked with SiN_3O tetrahedra [6], while the O′-sialon is a solid solution of Si_2N_2O and Al_2O_3 without changing both the orthorhombic structure of Si_2N_2O and the atomic ratio of metal/non-metal = 2/3 [7]. The general formula of O′-sialon is expressed as $Si_{2-x}Al_xO_{1+x}N_{2-x}$ with very limited solubility of aluminium and oxygen; various values have been reported for x ranging 0.05–0.6 as summarized by Trigg and Jack [8]. The lattice parameters of O′-sialon increase with increasing aluminium and oxygen contents [8–10] similar to the β′-sialon.

Both β′- and O′-sialon are often observed to coexist in sintered sialon ceramic. Phase stabilities of these two phases, therefore, have usually been studied by sintering. Recently, Mitomo *et al.* [11] related a thermal decomposition of Si_2N_2O to higher weight loss and higher porosity in reaction-sintered Si_2N_2O. They expressed the thermal decomposition of Si_2N_2O as $3\ Si_2N_2O\ (s) = Si_3N_4(s) + 3SiO\ (g) + N_2\ (g)$ as defined by Ehlert and co-workers [12, 13], and concluded that higher nitrogen pressure suppressed the thermal decomposition of Si_2N_2O. Because β′- and O′-sialon are often present in the sintered silicon nitride ceramics and considered as useful high-temperature engineering materials [7, 10, 14], the phase relationship of β′- and O′-sialon should be further elucidated under defined conditions. Furthermore, because β′-sialon whisker is a quite new material, its characteristics relative to the β′-sialon powder are not known. In this work, an equilibrium phase relationship between Area 3 β′-sialon whisker, Area 4 β′-sialon powder and Area 4 O′-sialon powder was investigated in the presence of graphite at 1623 K.

2. Experimental procedure

2.1. Synthesis

The synthesis procedure was the same as that published in the previous paper [4]. Starting materials

0022–2461 © *1993 Chapman & Hall*

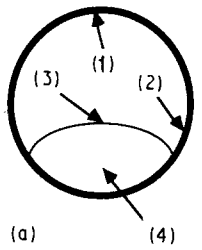

(1) α' >>> β' (whiskers)
(2) α' >> β' (whiskers)
(3) β' >>> α' (whiskers)
(4) O' ≈ β' (short whiskers and powders)

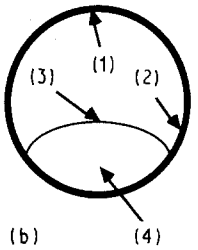

(1) α >>> β (whiskers)
(2) α >>> β (whiskers)
(3) α >>> β (whiskers)
(4) Si_2N_2O > α >>> β (short whiskers and powders)

Figure 1 Summary of phases formed in the four different areas with (a) Na_3AlF_6 and (b) NaF as the molten bath.

(3 g) with molecular ratio of $SiO_2/C/Na_3AlF_6 = 1/3/1$ were reacted with nitrogen gas at 1623 K. Reaction times were changed for 2, 7, 8 and 16 h.

2.2. Annealing

Several synthesized samples were further annealed at 1623 K for 8 h using the same arrangement as for synthesis. The purpose of annealing was to bring all phases involved to the equilibrium and to examine any changes before and after annealing in phase stabilities, compositions and crystallographic features. The following conditions were applied for the annealing.

1. β'-sialon whiskers were collected from Area 3 and β' and O' mixed powders from Area 4 after synthesis and designated Area 3 β'(w), Area 4 β'(p) and Area 4 O'(p), respectively. These three samples were placed in a graphite reaction tube and annealed. Four combinations were chosen for annealing: (1) β'(w) + β'(p), (2) β'(w) + β'(p) + O'(p), (3) β'(w) only, and (4) O'(p) only. The whiskers and powders were separated but sufficiently close to each other in the first and the second cases.

2. The samples were annealed with an additional graphite powder in the graphite reaction tube to ensure $a_C = 1$, where a_C is the activity of carbon.

3. Nitrogen gas was kept flowing until the temperature reached 1623 K, then the gas inlet was closed. Thus the solid samples and atmosphere gas would be close to equilibrium.

2.3. Characterization

Phases were identified by X-ray powder diffraction, using nickel-filtered CuK_α (Rigaku "Rotaflex"). The lattice parameters were calculated using a computer program (Rigaku D/Max) using pure silicon as an internal standard.

Quantitative microanalysis for the Al/Si ratio was performed using a Tractor-Northern Series II X-ray analyser attached to a TEM (Jeol 2000FX) operated at 200 kV. The Al/Si ratio was determined from intensities of AlK_α and SiK_α as

$$C_{Al}/C_{Si} = K_{Al\,Si}[I_{Al}/I_{Si}] \quad (1)$$

where C is the element wt %, I the characteristic X-ray intensity and K the Cliff–Lorimer factor. The value of K was determined as $K_{Al\text{-}Si} = 1.27 + 0.01$ from 15 measurements of Adularia ($KAlSi_3O_8$), whose composition had been analysed by EPMA (CAMEBAX-MICRO).

3. Results and discussion

3.1. As-synthesized samples

In the as-synthesized condition, Area 4 contains both O'- and β'-sialon powders as well as small amounts of β'-sialon short whiskers. Transmission electron micrographs in Fig. 2 show that the particle sizes of Area 4 O'-sialon powders were much finer than β'-sialon powders.

Relative amounts of β' and O' phases in Area 4 powders of as-synthesized samples depend on the reaction time. The XRD patterns of Area 4 powders of various reaction times are compared in Fig. 3. In the 2 h run, O'-sialon was the only detectable crystalline phase, with a considerable amount of amorphous phase being present. The amorphous phase has been identified as a remaining fluorosilicate, which appeared in a spherical shape and contained silicon, sodium and aluminium [3]. β'-sialon was identified in the 7 h reaction sample and then became the major phase in the 16 h sample, although a significant amount of O'-phase was still present, as seen in Fig. 3c. This β'-sialon was β'-sialon powder mixed with small amounts of short whiskers. It was also found that X-phase existed in the 7 h sample. Fig. 3 includes XRD data of a sample which was synthesized for 7 h followed by 8 h annealing, Fig. 3d. Only β'-sialon was found in this sample.

Effects of reaction time on the relative amounts of β' and O' phases in the Area 4 powder, [β'/O'] ratio, is estimated based on the peak heights of XRD patterns as follows

$$\beta'/O' = [I_{(100)} + I_{(110)} + I_{(200)} + I_{(101)} + I_{(210)}]^{\beta'}/[I_{(110)} + I_{(020)} + I_{(111)} + I_{(130)} + I_{(002)} + I_{(201)}]^{O'} \quad (2)$$

where I is the peak height of the corresponding index. The relative [β'/O'] ratio increases with reaction time, as shown in Fig. 4. These observations suggest that O'-sialon was formed during the early stages of synthesis, and then the β'-sialon increased with increasing reaction time. Changes in the [β'/O'] ratio with reaction time were in good agreement with changes in P_{O_2} [5]. p_{O_2} was measured at 1623 K by a ZrO_2 solid electrolyte during whisker synthesis. In an early stage of reaction, p_{O_2} reached a level of $10^{-11.5}$ atm as a result of enhanced carbothermal decomposition of silica. The O'-sialon was formed during this period, and then β'-sialon became the major phase as p_{O_2} decreased with reaction time.

The Si/Al atomic ratios analysed by X-ray energy spectrum are summarized in Table I with identified

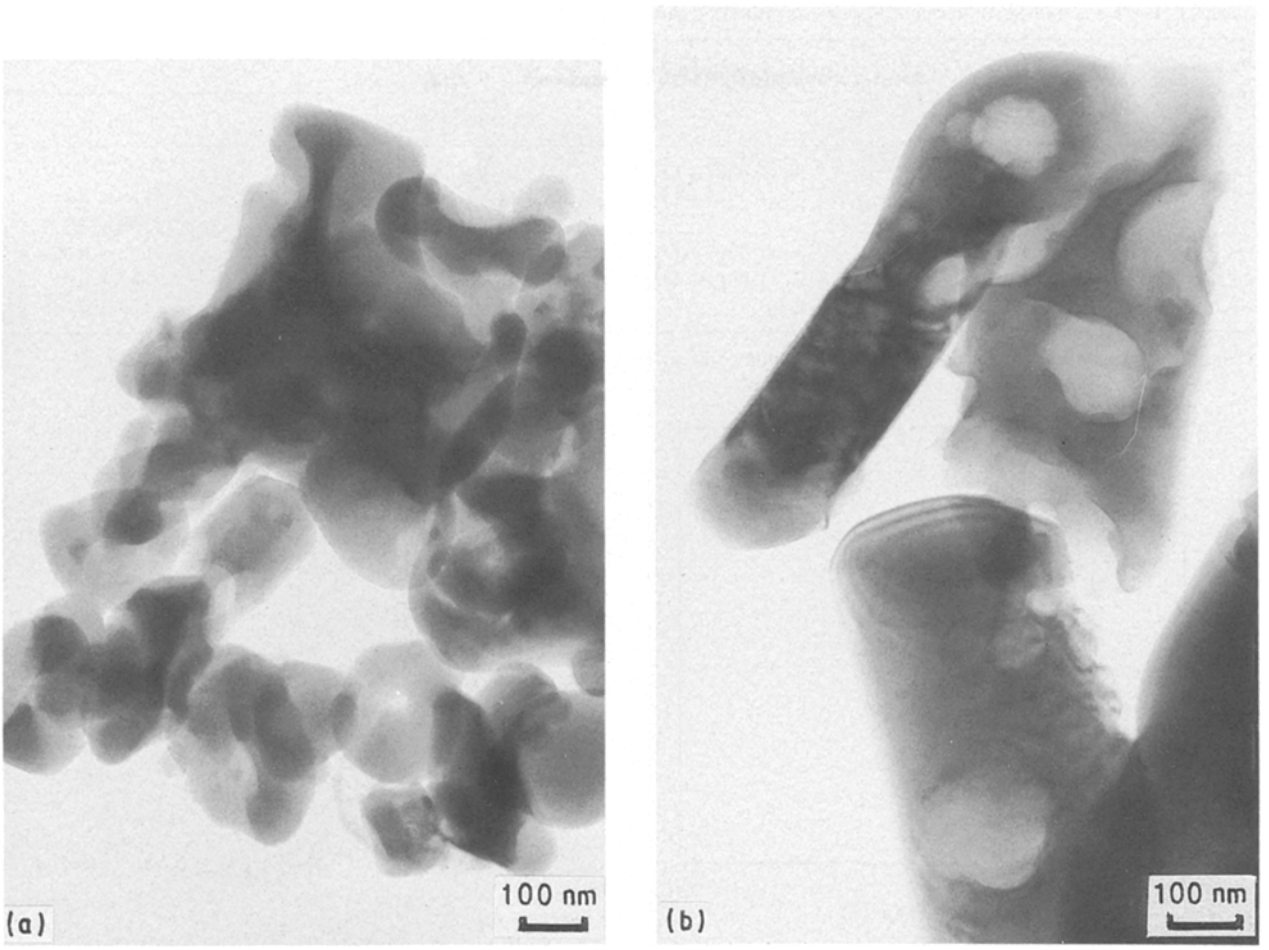

Figure 2 Transmission electron micrographs of Area 4 powders, (a) O′-sialon powder and (b) β′-sialon powder.

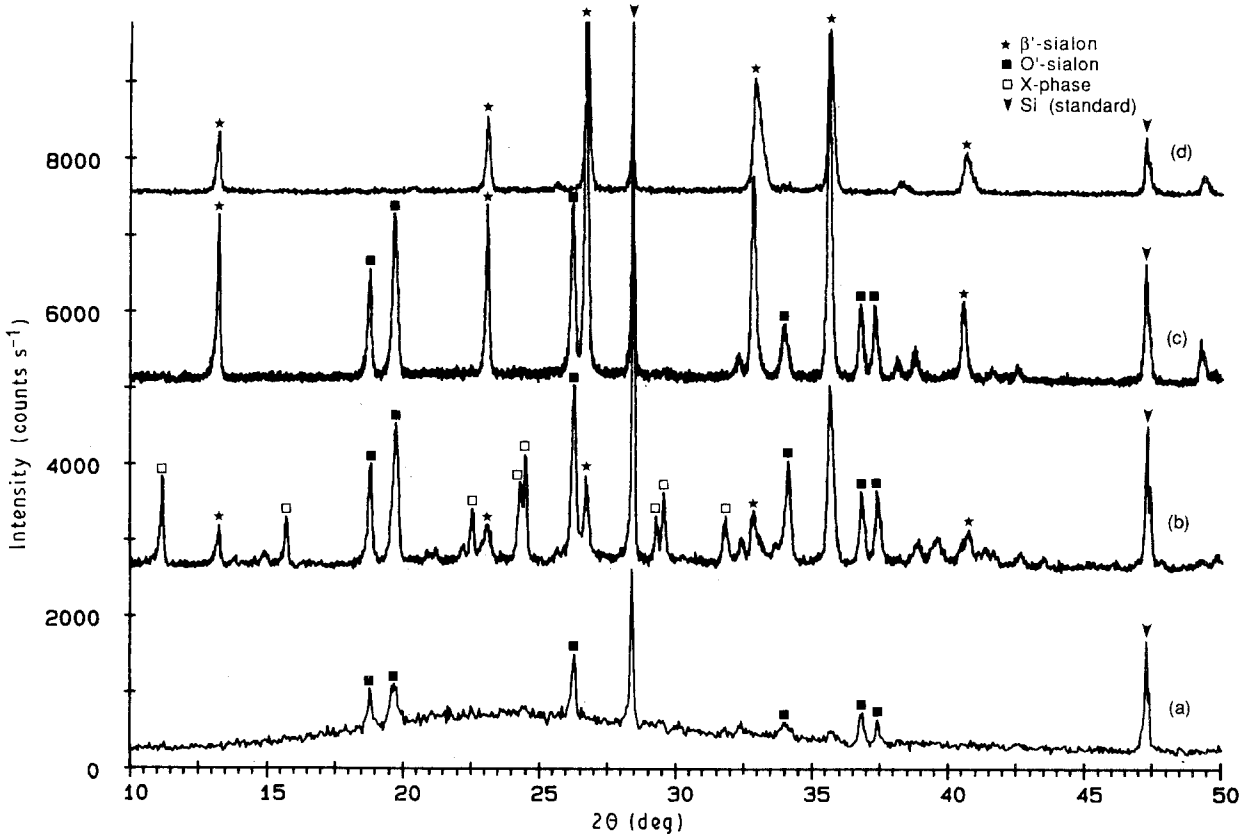

Figure 3 XRD patterns of samples of various reaction times: (a) 2 h, (b) 7 h, (c) 16 h and (d) 7 h reaction followed by 8 h annealing.

TABLE I. Phases and Si/Al atomic ratios of as synthesized samples

Reaction time (h)	N_2 flow rate ($cm^3\ min^{-1}$)	Phase identified	Si/Al atomic ratio		
			β′(w)	β′(p)	O′(p)
8	50	β′(w), β′(p) + O′(p)	5.19 ± 0.54		
7	100	β′(w), β′(p) + O′(p)	3.66 ± 0.29 3.70 ± 0.14[a]	1.61 ± 0.59	1.65 ± 0.33
8	100	β′(w), β′(p) + O′(p)		1.37 ± 0.11	1.72 ± 0.06
16	100	β′(w), β′(p) + O′(p)	2.41 ± 0.26	1.18 ± 0.13	1.63 ± 0.02
2	100	O′(p)			2.33 ± 0.16

[a] The Si/Al ratio was analysed after whiskers were thinned by a HF solution.

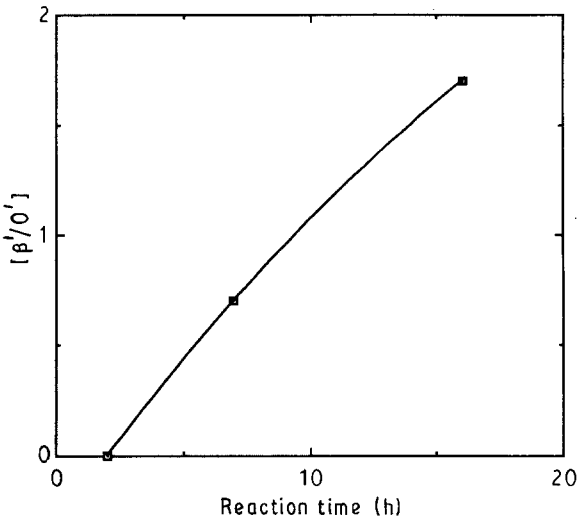

Figure 4 Changes in [β′/O′] ratio as a function of reaction time.

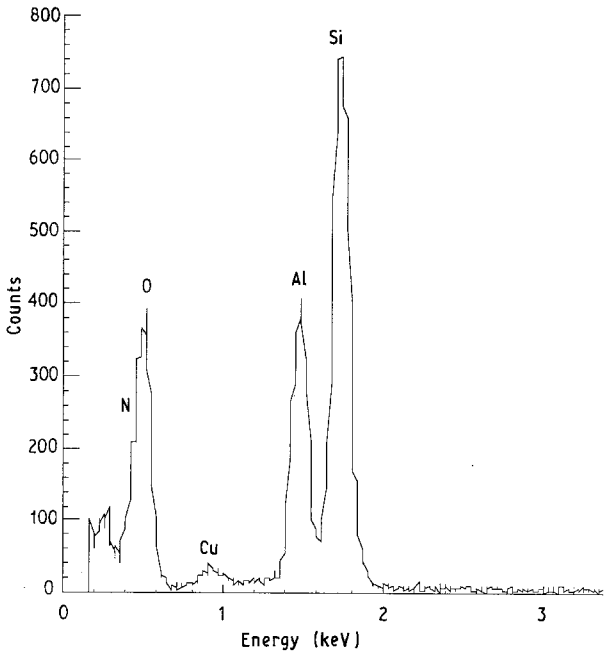

Figure 5 A typical X-ray energy spectrum of Area 4 O′-sialon powder.

phases for as-synthesized samples. These Si/Al ratios were determined by averaging several microanalyses. Table I shows that Area 3 β′-whiskers contain higher Si/Al ratios than Area 4 β′-powders of the same run. The aluminium content increases with higher nitrogen flow rates as well as longer reaction times in both β′-whisker and powder. It is particularly higher in the sample of the longest reaction time, 16 h: the 39 eq % Al of β′-powder is very close to that of β'_{40}.

No change was observed in the Si/Al ratios after about 0.1 μm of the surfaces were removed from the β′-whiskers by an HF–CH_3OH (1:5) solution. An example is included in Table I.

The O′-powder formed in the initial stage of synthesis contains relatively low aluminium, but after 7 h, its Si/Al ratio becomes fairly constant. A typical X-ray energy spectrum of as-synthesized O′-sialon powder is shown in Fig. 5. The spectrum shows a significantly high intensity of OK_α peak compared to β′-sialon [1]. The O′-sialon is not likely to contain sodium, because the sodium peak has never been observed in any X-ray energy spectra, while the lighter elements (oxygen and nitrogen) were observed as seen in Fig. 5. A copper peak in Fig. 5 is due to a copper grid used to support the O′-sialon powder sample.

3.2. Annealed samples

3.2.1. Phase stability

Table II summarizes results of microanalyses along with the phases identified in the charged and annealed samples. Four combinations of Area 3 β′(w), Area 4 β′(p) and Area 4 O′(p) were annealed: (1) β′(w) + β′(p), (2) β′(w) + β′(p) + O′(p), (3) β′(w) only and (4) O′(p) only. Because it was anticipated that the final Si/Al ratios would be controlled by the amounts of silicon, aluminium, nitrogen and oxygen available in the annealing system as well as the annealing condition, pairs were made with various Si/Al ratios. For instance, in case 1, β′(p) was paired with β′(w) of two different Si/Al ratios in Runs 1 and 2 as shown in Table II.

In Runs 1 and 2, no change in phases occurred by annealing. On the other hand, only β′(w) and β′(p) were identified after annealing in Runs 3 and 4 which were annealed with O′(p). In Run 5, β′(w) was the only phase annealed with graphite, while O′(p) with the highest Si/Al ratio was annealed without any other phases except graphite in Run 6. As shown in Table II, β′(w) and β′(p) were the only phases identified in the annealed samples of Runs 5 and 6, respectively.

Area 4 β′(p) usually contained a small amount of short β′-whiskers after the synthesis [4] as well as after the annealing. Fig. 6 shows scanning electron micrographs of charged O′(p) and of the same sample after annealing which was identified as β′(p) with short β′-whiskers. The morphology of the annealed sample

TABLE II. Changes in phases and Si/Al ratios by annealing

Run	Phases:	Si/Al atomic ratio				
	charged/resulted	Charged			Resulted	
		β′(w)	β′(p)	O′(p)	β′(w)	β′(p)
1	β′(w), + β′(p)/β′(w) + β′(p)	2.41 ± 0.26	1.18 ± 0.13		2.39 ± 0.21	1.20 ± 0.10
2	β′(w) + β′(p)/β′(w) + β′(p)	3.66 ± 0.29	1.18 ± 0.13		2.79 ± 0.19	1.86 ± 0.22
3	β′(w), + β′(p) + O′(p)/β′(w) + β′(p)	3.66 ± 0.29	1.61 ± 0.59	1.65 ± 0.33	2.56 ± 0.23	1.52 ± 0.32
4	β′(w), + β′(p) + O′(p)/β′(w) + β′(p)	5.19 ± 0.54	1.18 ± 0.13	1.63 ± 0.02	3.63 ± 0.23	Analysis failed
5	β′(w)/β′(w)[a]	3.66 ± 0.29			3.43 ± 0.30	
6	O′(p)/β′(p)[b]			2.33 ± 0.16		1.68 ± 0.16

β′(w): Area 3 β′-sialon whiskers, β′(p): Area 4 β′-sialon powders, O′(p): Area 4 O′-sialon powders.
[a]β′-sialon whiskers formed during annealing.
[b]β′-sialon powders formed during annealing.

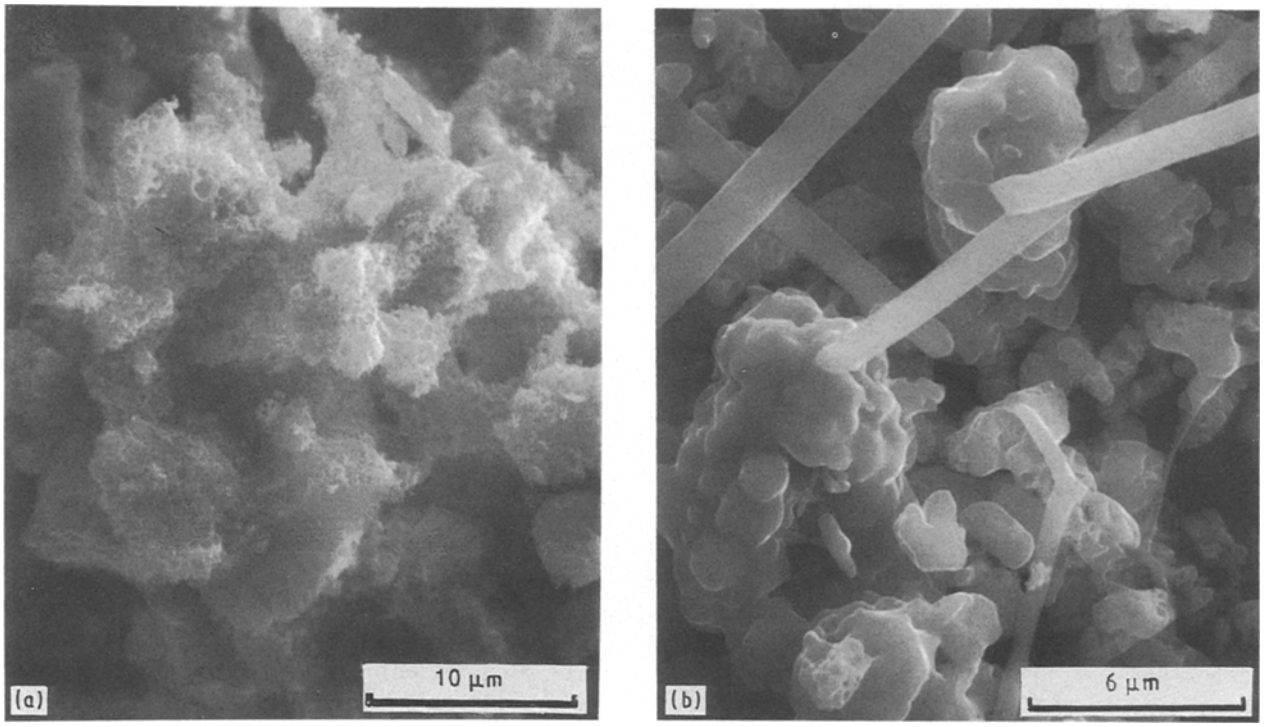

Figure 6 Scanning electron micrographs of (a) Area 4 O′-sialon powder with amorphous phase formed in an as-synthesized sample after 2 h reaction, and (b) β′-sialon powder with short whiskers formed from the O′-sialon shown in (a) in Run 6.

bears no relation to that of the original O′(p) which is an indication of reconstructive nature of O′-sialon/β′-sialon relation during annealing. In Fig. 7, a scanning electron micrograph of β′(p) formed from a β′(p) and O′(p) mixture in Run 3 is shown for comparison. Both β′-sialon powders shown in Figs 6b and 7 seem to have similar morphology and contain short whiskers regardless of their origins. It could be inferred from these results that the O′-phase is not a stable phase under the present annealing condition.

The formation of $Si_3N_4(\beta)$ and Si_2N_2O from SiO(g) in the Si–C–N–O system may be expressed as follows [1]

$$3SiO(g) + 3CO(g) + 2N_2(g) = Si_3N_4(\beta) + 3CO_2(g) \quad (3a)$$

$$2SiO(g) + CO(g) + N_2(g) = Si_2N_2O + CO_2(g) \quad (4a)$$

Because CO/CO_2 can reasonably be assumed in equilibrium during annealing as $CO_2(g) + C$ $(a_C = 1) = 2CO(g)$, overall reactions are rewritten as

$$3SiO(g) + 2N_2(g) + 3C = Si_3N_4(\beta) + 3CO(g) \quad (3b)$$

$$2SiO(g) + N_2(g) + C = Si_2N_2O + CO(g) \quad (4b)$$

Logarithms of activities of $Si_3N_4(\beta)$ and Si_2N_2O in the above reactions are expressed by the following equations

$$\log a_{Si_3N_4} = \log K_{3b} - 3\log p_{CO} + 3\log p_{SiO} + 2\log p_{N_2} + 3\log a_C \quad (3c)$$

$$\log a_{Si_2N_2O} = \log K_{4b} - \log p_{CO} + 2\log p_{SiO} + \log p_{N_2} + \log a_C \quad (4c)$$

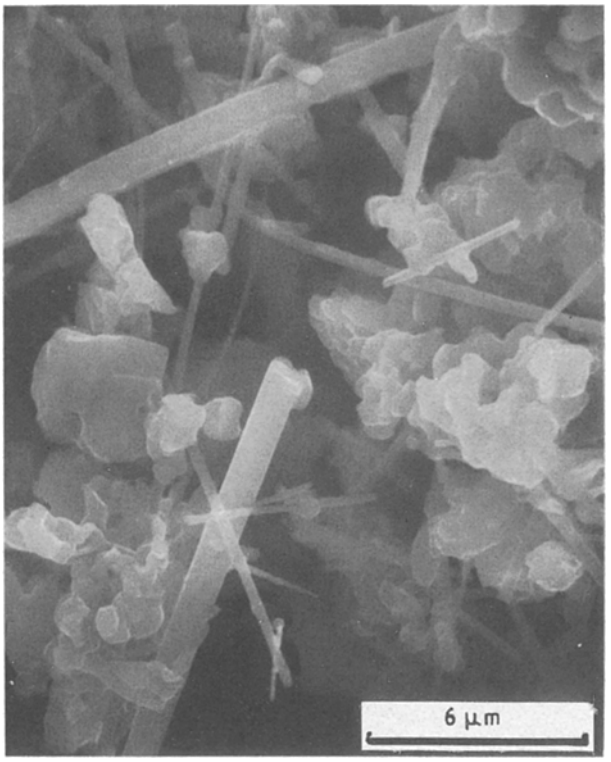

Figure 7 A scanning electron micrograph of β′-sialon powder with short whiskers formed from a mixed powder of β′- and O′-sialon in Run 3.

where K_{3b} and K_{4b} are the equilibrium constants of Equations 3b and 4b, respectively, which are evaluated as $\log K_{3b} = 49\,747/T - 22.88$ and $\log K_{4b} = 29\,211/T - 10.81$ [2].

If solid Si_3N_4(β) and Si_2N_2O are taken as the standard states, the two activities are $a_{Si_3N_4} = 1$ and $a_{Si_2N_2O} < 1$ when Si_3N_4 is the only stable solid phase, hence the difference of the two activities is larger than zero. At 1623 K and $a_C = 1$, it is expressed as

$$\{\log a_{Si_3N_4} - \log a_{Si_2N_2O}\} = 0.598 - 2\log p_{CO} + \log p_{SiO} + \log p_{N_2} > 0 \quad (5)$$

Equation 5 shows that the effects of CO and N_2 on the phase stability are opposite: higher p_{N_2} or lower p_{CO} increase the stability of Si_3N_4. It implies that Si_3N_4 is more stable at a lower p_{SiO}/p_{N_2} ratio when p_{O_2} is kept constant [2].

3.2.2. Decomposition of O′-sialon powder

Experimental results of annealing clearly showed that O′(p) was not a stable phase under the present annealing condition and it was decomposed. Because nitrogen was kept at $p_{N_2} = 1$ atm and the CO/CO_2 ratio was expected to be in equilibrium during the annealing, the disappearance of O′(p) could be expressed by

$$Si_{2-x}Al_xO_{1+x}N_{2-x} + (3x/2 - 1)CO(g) = (2 - x)SiO(g) + (1 - x/2)N_2(g) + (3x/2 - 1)CO_2(g) + (x/2)Al_2O(g) \quad (6)$$

Although how the aluminium- and oxygen-containing species moved from O′ to β′ is not clear, $Al_2O(g)$ has been identified as the highest partial pressure over the Al_2O_3–Si and Al_2O_3–Al mixtures under the reducing conditions [15, 16]. Released $Al_2O(g)$ may be related to the increase of aluminium content in β′-sialon whiskers.

3.2.3. Si/Al ratio

Changes in the Si/Al ratios in β′ and O′ phases are plotted in Fig. 8, where two curves are drawn for β′ and O′-sialons by assuming general formulas for both phases. x is an indication of the dissolutions of aluminium and oxygen in sialons. Si/Al ratios for β′(w), β′(p) and O′(p), obtained in the same as-synthesized sample are connected with dotted lines. Si/Al ratios measured after annealing are connected to the charged valves with arrows. The Si/Al ratio is always higher in β′-sialon whiskers than in powder both in as-synthesized and annealed samples. Because annealing was carried out in a closed manner, the final Si/Al ratios of β′(w) and β′(p) depended on the Si/Al ratios and amounts of phases in charged materials. The Si/Al ratios remained the same level in Run 1 where β′(w) and β′(p) samples were annealed after 16 h synthesis. On the other hand, if β′(w) was replaced with other whiskers of lower aluminium content as Run 2, or O′(p) was included in annealing as in Run 3 or Run 4, aluminium increased in β′(w), while it decreased in β′(p). The Si/Al ratios were much closer in β′(w) and β′(p) after annealing. Fig. 8 clearly indicates that the majority of aluminium and oxygen released from the decomposing O′(p) was probably incorporated into whiskers. The ratios remained practically unchanged in β′(w) if it was annealed alone, as seen in Run 5. The ratios showed little change in β′(p) except in Run 2, where β′(p) of higher aluminium content was annealed with β′(w) of much lower aluminium content.
nium content.

The aluminium contents of β′(w) and β′(p) were closer after annealing, but they never reached the

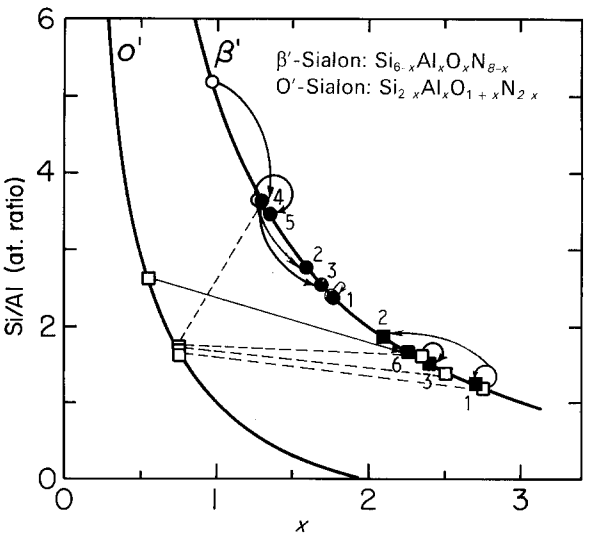

Figure 8 Relationships between Si/Al ratio and x in β′-sialon and O′-sialon. Si/Al ratios for (○) β′(w), (□) β′(p) and O′(p) as-synthesized, and (●) β′(w), (■) β′(p) after annealing. The numbers indicate the Run number in Table II.

same value: the aluminium contents were always lower in the β′(w). For example, in Run 3, x was higher in the β′(p) by as much as 0.7 even after x was increased 30% in β′(w) by annealing. Although the (Si–N)/(Al–O) replacement or accommodation of aluminium and oxygen during annealing are not well understood, these can only occur if there is an overall decrease in the energy of the system by the replacement/accommodation. However, whether the observed difference in aluminium contents in β′(w) and β′(p) is related solely to their morphologies or rather kinetically controlled, is not clear at this point.

3.3. Lattice parameters

A change in the lattice parameter with a changing composition of solid solution is directly related to the change of the atomic distance as a result of atom replacement. Fig. 9 shows the relationship between lattice parameters and x for β′(w) and β′(p), and compared with other measurements [7, 17, 18]. The lattice parameters of the same whiskers before and after annealing, and those of powders, are shown. If β′(w) was annealed alone, or together with β′(p) which was synthesized in the same run, its lattice parameters and x remained practically the same after annealing. In all other cases, its lattice parameters remained unchanged while x increased: the aluminium content and probably O increased without changing its structure. On the other hand, both parameters decreased in β′(p) while aluminium remained unchanged except in Run 2, where β′(p) of higher aluminium was annealed with β′(w) of much lower aluminium content and without O′(p). The lattice parameters of β′(p) formed from O′(p) in Run 6 are in reasonable agreement with those of Run 3, which also included O′(p).

The fact that x increased in β′(w) when its lattice parameters remained practically the same could be caused by the (Si–N)/(Al–O) replacements. The bond lengths have been reported to be (Si–O) ~ 0.161 nm, (Si–N) ~ 0.174 nm, (Al–O) ~ 0.175 nm and (Al–N) ~ 0.187 nm [6, 8]. Therefore, replacing an (Si–N) bonding with an (Al–O) bonding would increase the aluminium content of β′(w) but change its lattice parameters very little. The β′(w) was synthesized in Area 3 where aluminium and oxygen were lower than in Area 4 where β′(p) was formed. β′(w) contained lower aluminium and oxygen after synthesis and should be able to accommodate more aluminium and oxygen during annealing without a structural adjustment up to a certain limit. β′(p), on the other hand, underwent a restructuring without compositional change of aluminium up to a certain limit.

After annealing, lattice parameters of β′(w) and β′(p) become much closer. For instance, Δa and Δc are less than 1% in Run 2 which shows the largest difference in the lattice parameters, while Δx is about 30%. Because bond lengths are longer in nitrogen-containing bonds, β′(w) may contain more nitrogen-containing bonding than β′(p), due to its ⟨2 1 0⟩ growth directions. As seen in Fig. 9, the lattice parameters of β′(w) measured in the present work are much higher than the three lines, although the parameters are closer to the lines after annealing. Three references were based on the sintered samples and the values of

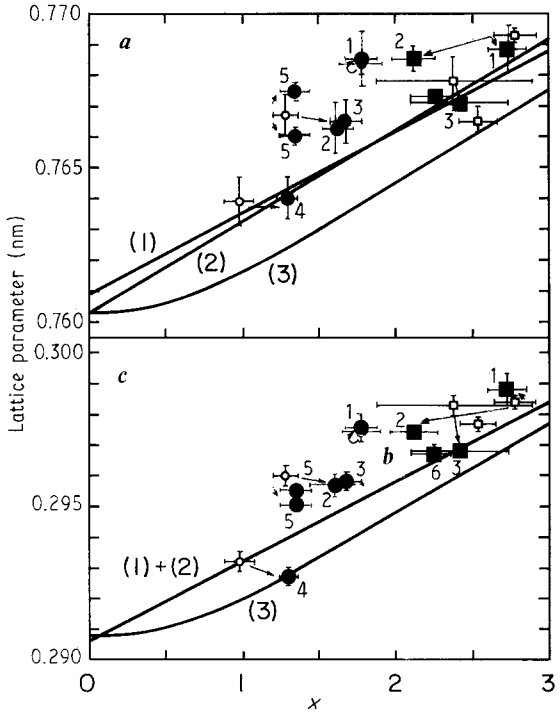

Figure 9 Lattice parameters of β′-sialon as a function of x. (○) Whiskers in as-synthesized samples, (●) whiskers in annealed samples, (□) powders in as-synthesized samples, and (■) powders in annealed samples. (1) [17], (2) [18], (3) [7].

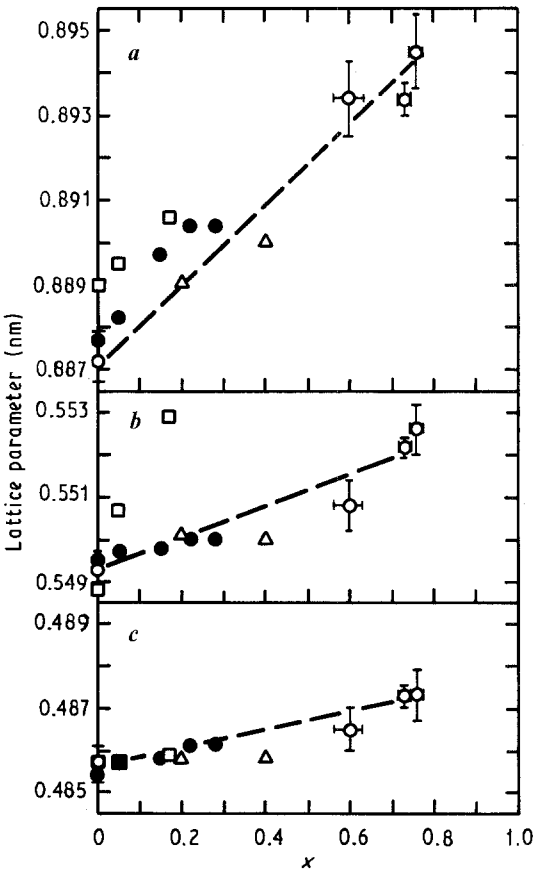

Figure 10 Lattice parameters of O′-sialon as a function of x. (○) Present study, (●) [8], (□) [9], (△) [10].

x were calculated from the nominal compositions of starting materials.

In Fig. 10, the measured lattice parameters of as-synthesized O′(p) are compared with other measurements [8–10], in which O′-sialon was made by sintering at higher temperatures and the x values were determined based on the nominal compositions of starting materials. An increase in the lattice parameters a, b and c of O′-sialon with the increasing aluminium and oxygen contents was first reported by Naik *et al.* [9]. An increase in a with increasing x was much larger than those found in b and c. Trigg and Jack [8] reported that the change in a was approximately five times that of b. The same trend was also reported by Yamai and Ota [10]. The lattice parameters of Si_2N_2O (i.e. $x = 0$) were determined as $a = 0.8872(5)$ nm, $b = 0.5493(4)$ nm and $c = 0.4857(4)$ nm from the measurements on Si_2N_2O formed with NaF as the molten bath in this study, which were in good agreement with the reported values [8, 19, 20].

As pointed out by Idrestedt and Brosset [6], the Si_2N_2O structure has two special features: (1) the oxygen atoms are located in the layers perpendicular to the [1 0 0] direction and (2) the silicon and nitrogen atoms form a parallel layer between two oxygen layers. The lattice parameters of Si_2N_2O along the a direction are constructed mainly of (Si–O) bonds, while (Si–N) bonds are the main constituents for determining the parameters along the b and c directions. The replacements of silicon and nitrogen with aluminium and oxygen would make the following changes: (Si–O) would be replaced by (Al–O) along the a direction, and (Si–N) replaced by (Al–O) along the b and c directions. The increment of the average bond length in the a direction with the (Si–O)/(Al–O) replacement is, therefore, expected to be much larger than in other directions.

The highest value of x in O′-sialon was generally believed to be less than 0.3 [8]. However, the present study shows that the x value could be as high as 0.76 under certain conditions, resulting in significantly larger lattice parameters. The values of x were determined by averaging several Si/Al ratios obtained by microanalysis on individual O′-sialon particles in the present work.

4. Conclusions

1. β′-sialon is a stable phase at 1623 K, $a_C = 1$ and $p_{N_2} = 1$ atm, but O′-sialon is not a stable phase.

2. O′-sialon is formed in Area 4 during the synthesis because of a higher p_{O_2}. It becomes less stable during the annealing under low p_{O_2} as well as high p_{CO}/p_{CO_2} ratio, and decomposes as

$$Si_{2-x}Al_xO_{1+x}N_{2-x} + (3x/2 - 1)CO(g) = (2 - x)SiO(g) + (1 - x/2)N_2(g) + (3x/2 - 1)CO_2(g) + (x/2)Al_2O(g)$$

3. The lattice parameters of β′-sialon whiskers remain unchanged before and after annealing, despite increasing aluminium contents. The most likely reaction during the annealing is (Si–N)/(Al–O) replacement.

Acknowledgement

The research was supported by The National Science Foundation through MSM-8719951.

References

1. H. WADA and M. J. WANG, in "Proceedings of the International Conference on Whisker- and Fiber-Toughened Ceramics," edited by R. A. Bradley, D. E. Clark, D. C. Larsen and J. O. Stiegler (ASM International, 1988) p. 63.
2. H. WADA, in "Proceedings of the International Symposium on Advances in Processing and Application of Ceramic and Metal Matrix Composites," edited by H. Mostaghaci, (Pergamon Press, 1989) p. 3.
3. M. J. WANG and H. WADA, in "Preparation and Properties of Silicon Nitride Based Materials", edited by D. A. Bonnell and T. Y. Tien (Trans Tech, 1989) p. 267.
4. *Idem, J. Mater. Sci.* **25** (1990) 1690.
5. H. WADA and L. WANG, *ibid.* **27** (1992) 1528.
6. I. IDRESTEDT and C. BROSSET, *Acta Chem. Scand.* **18** (1964) 1879.
7. K. H. JACK, *J. Mater. Sci.* **11** (1976) 1135.
8. M. B. TRIGG and K. H. JACK, *J. Mater. Sci. Lett.* **6** (1987) 407.
9. I. K. NAIK, L. J. GAUCKLER and T. Y. TIEN, *J. Amer. Ceram. Soc.* **61** (1978) 332.
10. I. YAMAI and T. OTA, *Adv. Ceram. Mater.* **2** (1987) 784.
11. M. MITOMO, S. ONO, T. ASAMI and S. L. KANG, *Ceram. Int.* **15** (1989) 345.
12. T. C. EHLERT, T. P. DEAN, M. BILLY and J. C. LABBE, *J. Amer. Ceram. Soc.* **63** (1980) 235.
13. M. BILLY, J. C. LABBE and P. LORTHOLARY, *Mater. Chem.* **4** (1979) 189.
14. M. E. WASHBURN, *Amer. Ceram. Soc. Bull.* **46** (1967) 667.
15. G. GRUBE, A. SCHNEIDER, U. ESCH and M. FLAD, *Z. Anorg. Chem.* **260** (1949) 120.
16. L. BREWER and A. W. SEARCY, *J. Amer. Chem. Soc.* **73** (1951) 5308.
17. H. HOHNKE and T. Y. TIEN, in "Progress in Nitrogen Ceramics", edited by F. L. Riely (Martinus Nijhoff, 1983) p. 101.
18. T. EKSTROM, P. O. KALL, M. NYGREN and P. O. OLSSON, *J. Mater. Sci.* **24** (1989) 1853.
19. P. MORGAN, JCPDS 33-1161, Powder Diff, File (International Centre for Diffraction Data).
20. C. M. B. HENDERSON and D. TAYLOR, *Trans. Br. Ceram. Soc.* **74** (1975) 49.

Received 6 August 1991
and accepted 7 May 1992